Density profiles in a diphasic lattice-gas model

C. Appert* and D. d'Humières†
Laboratoire de Physique Statistique, CNRS URA 1306, École Normale Supérieure, 24 rue Lhomond, 75231 Paris Cedex 05, France
(Received 23 August 1994)

We predict the density profile across a flat interface created in lattice-gas models by the introduction of an attractive interaction. The resulting theoretical equilibrium densities and surface tension are in good agreement with direct simulations of the model.

PACS number(s): 47.55.Kf, 05.70.Fh, 05.50.+q, 05.70.Ln

I. INTRODUCTION

In 1986, Frisch, Hasslacher, and Pomeau proposed a lattice-gas model for studying hydrodynamics [1]. It is a fictitious gas made of pointlike particles moving on a lattice, which obeys Navier-Stokes equations in the incompressible limit. As semidetailed balance is verified by the microscopic evolution rules, it has been proved in the frame of the Boltzmann assumption (correlations are neglected) that there exists a unique uniform equilibrium distribution of Fermi-Dirac form [2,3].

In this paper, we address such a lattice-gas model, to which has been added an attractive interaction between particles [4]. This force mimics the cohesion forces of a liquid and creates a phase separation into two phases of different densities. The interaction is purely dynamically defined and is irreversible. Then the system evolves irreversibly in the phase space until it reaches a subspace where it is dynamically trapped. For our choice of the interaction, the attractor of this dynamical system corresponds to a separated state for a certain range of the parameters. The model will be referred to as the liquid-gas model.

An alternative approach could have been to use a thermal lattice gas [5] and to introduce an attractive interaction potential. Then the equilibrium state would have been governed by the minimization of a free energy. Although the latter approach would have more traditional thermodynamical properties, it yields more complicated models. The model studied here, as well as similar models [6], may be considered as minimal models to simulate phase transitions in hydrodynamical systems.

Now the challenge is to build a theory for these models without using semidetailed balance, which is broken by the irreversibility of the attractive interaction. This study is akin to recently increasing efforts devoted to theories for systems which violate the basic assumptions of standard equilibrium thermodynamics [7–9].

In previous studies of the liquid-gas model [10], hydrodynamical equations governing the fluid behavior in each homogeneous phase have been calculated. We have also obtained an equation of state of the van der Waals type. However until now there was no way to predict equilibrium densities. These cannot be found from Maxwell's construction as the usual thermodyanmics fail here. Indeed, Shan and Chen [11] have shown that Maxwell's construction is not verified except for a very specific class of interaction forces. On the other hand, we have observed on numerical simulations that some important features of real systems are preserved in the liquid-gas model. Equilibrium densities seem unique. For a curved interface, Gibbs-Thomson relations which relate the equilibrium pressures on each side of the interface to the curvature and the equilibrium pressure for a flat interface are verified, even if the usual proof [12] cannot be performed anymore.

The aim of this paper is to present a theoretical prediction of the density profile across a fat interface—and thus of equilibrium densities and surface tension—using only dynamical arguments. Surface tension has already been predicted for the lattice-gas model of Rothman and Keller [13]. The difference here comes from the introduction of nonlocal evolution rules which modify deeply the solution method.

We will consider a flat interface at rest. An asymptotic first-order calculation has already been published [14]. Here we present a more complete study. Throughout the whole paper correlations will be neglected. We assume also that an equilibrium distribution exists for this problem, but its shape is not determined *a priori*. Actually, as the attractive interaction violates a semidetailed balance, equilibrium distributions are not bound to be Fermi-Dirac ones. A counterexample has been given by Bussemaker and Ernst for another lattice-gas model with biased collision rules [15].

In the first part of this paper, the reader will find the definition of the liquid-gas model in two and three dimensions. Then in Sec. V A a recurrence method will be used to predict the density profile and surface tension. The results will be compared with measurements on numerical simulations.

II. DEFINITION OF THE LIQUID-GAS MODEL

Let us first review the definition of the model in two dimensions [14,16]. As proposed by Frisch, Hasslacher, and Pomeau (FHP) [1], we consider point particles moving

*Electronic address: appert@physique.ens.fr
†Electronic address: dominiq@physique.ens.fr

from node to node on a hexagonal lattice, and colliding when they meet at a node. Particles may take seven velocities $\{\mathbf{c}_i\}_{i=1 \text{ to } 7}$. Six of them correspond to the directions of the lattice, and the last one is zero. The nonzero velocity modulus is such that, at each time step, moving particles hop to nearest-neighbor sites. This fictitious gas obeys an exclusion principle: at most one particle with a given velocity may occupy a given site at a given time. Then the occupation state of a site $\mathbf{x}$ may be represented as a boolean vector $n(\mathbf{x}) = \{n_i / i = 1 \text{ to } 7\}$. The symmetries of the system, together with mass and momentum conservation, ensure that the fluid obeys Navier-Stokes equations in the incompressible limit [2].

In order to produce phase separation into dense and light phases, we add an attractive interaction mimicking the cohesion forces in a liquid. The definition of the latter is purely dynamical, and not derived from a given potential. The idea is to take pairs of particles separated by a distance r and moving away from each other, and to send them back toward each other. The distance r is called the range of the interaction. At a microscopic scale, the evolution equation reads

$$\begin{aligned} n'_i(\mathbf{x},t) &= n_i(\mathbf{x},t) + \delta_i(n(\mathbf{x},t)) \\ n_i(\mathbf{x}+\mathbf{c}_i, t+1) &= n'_i(\mathbf{x},t) + \gamma_i - \gamma_{-i} \ , \end{aligned} \tag{1}$$

where δ_i is the collision operator and γ_i is a nonlocal operator set for the interaction between sites $\mathbf{x}$ and $\mathbf{x} + r\mathbf{c}_i$. It acts on postcollision configurations $\{n'_i(\mathbf{x},t)\}$

$$\gamma_i = n'_{-i}(\mathbf{x})[1 - n'_i(\mathbf{x})][1 - n'_{-i}(\mathbf{x}+r\mathbf{c}_i)]n'_i(\mathbf{x}+ri\mathbf{c}_i) \ , \tag{2}$$

with $\mathbf{c}_{-i} = -\mathbf{c}_i$. These rules define the so-called minimal model, in contrast to a previous more complicated version called the maximal model [17], which will not be described here.

The long range interaction is irreversible; it is always attractive and never repulsive. Then for certain values of the parameters the system may be driven toward a subspace of the phase space corresponding to separated phases. Indeed, starting from a uniform density, phase separation is observed in simulations [14].

As the interaction involves only velocities parallel to the interaction direction, the result is independent of the order in which interaction directions are explored. It is also independent of the order in which pairs of sites are explored in one given direction. Therefore, it is equivalent to performing the interaction sequentially or in parallel on all pairs in all directions. This was not the case for previous versions of the liquid-gas model. The simplification of the rules has allowed to extend the model to three dimensions (3D) [10,14]. We simply add the interaction defined by Eq. (1) to the face-centered hypercubic (FCHC) model [18]. We have used the algorithm of Rem and Somers to reduce the size of the collision table [19]. Collisions verify semidetailed balance. Some examples of three-dimensional decompositions are shown in [14].

III. DEFINITION OF THE PROBLEM

A. Boltzmann equation

The macroscopic behavior of a lattice gas results from the average of microscopic events. Thus in the theoretical approach we will replace the boolean variables $n_i(\mathbf{x})$ by the probabilities $N_i(\mathbf{x})$ of finding a particle at site $\mathbf{x}$ with the velocity $\mathbf{c}_i$.

We define b as the total number of velocity states in one given site, and b_m as the number of nonzero velocity states. Symbols with a hat denote vectors in the space of velocity states, for instance $\hat{\mathbf{N}}(\mathbf{x}) = \{N_i(\mathbf{x})\}_{i=1 \text{ to } b}$.

The evolution equation for probability distributions is called a Boltzmann equation, and is obtained by performing an ensemble average (noted $\langle\rangle$) on the microdynamical evolution equation (1). We neglect the correlations as postulated by the Boltzmann assumption. Thus probabilities are independent.

The evolution may still be decomposed into three stages—collisions, interactions, and propagation. A distribution $\hat{\mathbf{N}}$ becomes, after collisions,

$$\hat{\mathbf{N}}' = \hat{\mathbf{N}} + \hat{\mathbf{\Delta}}(\hat{\mathbf{N}}) \ , \tag{3}$$

and, after interactions,

$$\hat{\mathbf{N}}'' = \hat{\mathbf{N}}' + \hat{\mathcal{G}}(\hat{\mathbf{N}}') \tag{4}$$

where $\hat{\mathcal{G}}$ is a nonlocal operator defined by

$$\begin{aligned} \mathcal{G}_i &= \Gamma_i - \Gamma_{-i} \ , \\ \Gamma_i[\hat{\mathbf{N}}'] &= [1 - N'_i(\mathbf{x})]N'_{-i}(\mathbf{x})[1 - N'_{-i}(\mathbf{x}+r\mathbf{c}_i)] \\ &\quad \times N'_i(\mathbf{x}+r\mathbf{c}_i) \ . \end{aligned} \tag{5}$$

Then propagation reads

$$N_i(\mathbf{x}+\mathbf{c}_i, t+1) = N''_i(\mathbf{x},t) \ . \tag{6}$$

$\hat{\mathbf{\Delta}}$ and $\hat{\mathbf{\Gamma}}$, respectively, are the ensemble averages of the microdynamical collision and interaction operators

$$\Delta_i = \langle \delta_i \rangle \ , \tag{7}$$

$$\Gamma_i = \langle \gamma_i \rangle \ . \tag{8}$$

B. Description of the problem and symmetries

In what follows we consider steady flat interfaces. In a previous first-order calculation [14], the probability distribution was assumed to depend only on the coordinate x normal to the interface:

$$N_i(\mathbf{x}) = f(x) \, \forall i \ . \tag{9}$$

Here we relax this assumption and allow the probability distribution $N_i(\mathbf{x})$ also to depend on the velocity direction i:

$$N_i(\mathbf{x}) = N_i(x) \, \forall i \ . \tag{10}$$

By symmetry the system is invariant in directions parallel to the interface. To simplify, we will address only the case where all nonzero velocities have the same modulus c and the interface is such that c_{ix} can take only three different values $c_+, 0, c_- = -c_+$. This implies that the following calculation will apply for the FHP and FCHC models only for specific orientations of the interface. Using cristallographic notations, for FHP the interface must be parallel to $(1,0)$ and for FCHC it must be normal to $(1,0,0,0)$. For i such that $c_{ix} > 0$, we note $\mathcal{G}_+ = \mathcal{G}_i$ and $\Gamma_+ = \Gamma_i$.

We also restrict our study to models having no more than one rest particle per site, i.e., $b = b_m$ or $b_m + 1$. We will now summarize some additional notations that will be used in the paper. A synthesis is given in Table I.

The speed of sound c_s is given by

$$c_s^2 = b_m c^2 / bD \,, \tag{11}$$

where D is the dimension of space. Note that the FCHC model is in fact a four-dimensional (4D) model projected on 3D [18], and thus $D = 4$.

The number b_+ of forward velocities ($c_{ix} > 0, c_{ix} = c_+$) and c_+ will be determined from the two relations

$$\sum_{c_{ix}>0} c_{ix}^2 = b_+ c_+^2 \quad \text{and} \quad \sum_{c_{ix}>0} c_{ix}^4 = b_+ c_+^4 \,. \tag{12}$$

The symmetries of the FHP and FCHC lattices impose that [2]

$$\sum_{c_{ix}>0} c_{ix}^2 = \tfrac{1}{2} \sum_i c_{ix}^2 = \frac{b_m c^2}{2D} \tag{13}$$

and

$$\sum_{c_{ix}>0} c_{ix}^4 = \tfrac{1}{2} \sum_i c_{ix}^4 = \frac{3 b_m c^4}{D(D+2)} \,. \tag{14}$$

Thus

$$b_+ = \frac{D+2}{6D} b_m \quad \text{and} \quad c_+^2 = \frac{3}{D+2} c^2 \,. \tag{15}$$

Some useful relations on velocities are given in Appendix A.

TABLE I. Numerical values of the parameters for the FHP and FCHC models.

Parameter	Numerical values	
	FHP III model	FCHC model
D	2	4
b	7	24
b_m	6	24
b_+	2	6
c_+	$\sqrt{3}/2$	1
c_s	$\sqrt{3/7}$	$1/\sqrt{2}$
$\sum_{c_{ix}>0} c_{ix}^2$	3/2	6
$\sum_{c_{ix}>0} c_{iy}^2$	1/2	2
$\frac{1}{2}\sum_{c_{ix}=0} c_{iy}^2$	1	4

IV. SYMMETRIES OF THE SYSTEM

In this section we show that, due to the symmetries of the system and the assumption of stationarity, the distribution $\hat{\mathbf{N}}$ is a Fermi-Dirac distribution. This was not obvious *a priori*, as interactions do break the semidetailed balance.

A. Decomposition on eigenvectors

The probability distribution $\hat{\mathbf{N}}(x)$ can be decomposed on the basis of eigenvectors of the collision operator. In the present case, the expression can be simplified, as the system is invariant by any isometry leaving the x axis invariant. Among the 24 eigenvectors, only four are invariant by this set of transformations (Appendix B). Thus the generic form for any distribution $\hat{\mathbf{N}}$ having the symmetries of the system is

$$\hat{\mathbf{N}}(x) = f(x)\hat{\mathbf{1}} + h(c)\hat{\mathbf{C}}_x + q(x)\hat{\mathbf{Q}}_{xx} + (b - b_m)w(x)\hat{\mathbf{W}} \,, \tag{16}$$

with $Q_{i\alpha\beta} = c_{i\alpha}c_{i\beta} - (c^2/D)\delta_{\alpha\beta}$ and $W_i = 1$ for $i = 1$ to b_m, and $W_0 = -b_m$ if $b = b_m + 1$. We recall that $\hat{\mathbf{N}}(x)$, $\hat{\mathbf{1}}$, $\hat{\mathbf{C}}_x$, $\hat{\mathbf{Q}}_{xx}$, and $\hat{\mathbf{W}}$ stand for vectors in the space of velocity states. Notice that $\sum_i N_i(x) = bf(x)$. Then $f(x)$ is indeed the reduced density in site x.

B. First step in the calculation of the collision term

As any distribution having the symmetries of the system $\hat{\mathbf{\Delta}}(\hat{\mathbf{N}})$ may be written in the form

$$\hat{\mathbf{\Delta}}(\hat{\mathbf{N}}) = f'\hat{\mathbf{1}} + h'\hat{\mathbf{C}}_x + q'\hat{\mathbf{Q}}_{xx} + (b - b_m)w'\hat{\mathbf{W}} \,. \tag{17}$$

Moreover, collisions conserve mass and momentum

$$\sum_i \Delta_i(\hat{\mathbf{N}}) = 0 \,, \tag{18}$$

$$\sum_i \Delta_i(\hat{\mathbf{N}})\mathbf{c}_i = \mathbf{0} \,. \tag{19}$$

These relations imply, respectively, that $f' = 0$ and $h' = 0$, and thus

$$\hat{\mathbf{\Delta}}(\hat{\mathbf{N}}) = q'\hat{\mathbf{Q}}_{xx} + (b - b_m)w'\hat{\mathbf{W}} \,. \tag{20}$$

C. Final form of the collision operator

As it has been explained in Sec. III B, we consider the case where c_{ix} can take only three different values $(0, c_+, c_-)$. From Eq. (16), N_i can take only four different values corresponding to zero and nonzero velocities parallel to the interface, forward, or backward. We denote these values by N_0, $N_\parallel$, N_+, and N_-.

We are looking for a stationary solution of (6). For the

velocities parallel to the interface, it reads

$$N_{\|}^{t}(x) = N_{\|}^{t+1}(x) \quad \text{and} \quad N_{0}^{t}(x) = N_{0}^{t+1}(x) \qquad (\text{if } b = b_m + 1) \quad (21)$$

or

$$N_{\|}(x) = N_{\|}''(x) \quad \text{and} \quad N_{0}(x) = N_{0}''(x) \; . \qquad (22)$$

We replace N'' by its expression (4). Then

$$(b - b_m) w'(x) \hat{W}_{\|} + q'(x) Q_{xx\|} + \mathcal{G}_{\|}(\hat{\mathbf{N}}')(x) = 0 \; ,$$

$$(b - b_m) w'(x) \hat{W}_{0} + q'(x) Q_{xx0} + \mathcal{G}_{0}(\hat{\mathbf{N}}')(x) = 0 \; .$$

As $Q_{xx\|} = c^2/D$, $Q_{xx0} = 0$, $\hat{W}_{\|} = 1$, $\hat{W}_0 = -b_m$, and $\mathcal{G}_{\|} = \mathcal{G}_0 = 0$, we find $q' = w' = 0$, which implies that

$$\hat{\mathbf{\Delta}}(\hat{\mathbf{N}}) = \hat{\mathbf{0}} \; . \qquad (23)$$

The collision operator is the same as for the FHP or FCHC models without interactions. Then we know that (again, if correlations are neglected) the only distribution verifying Eq. (23) is the Fermi-Dirac equilibrium distribution [2,3]. This result will be used in Appendix C. It will completely determine q and w as functions of f and h.

Indeed, as for a Fermi-Dirac distribution $N_0 = N_{\|}$, it can immediately be seen that if $b = b_m + 1$ we have

$$w = \frac{c^2}{D(1 + b_m)} q \; . \qquad (24)$$

The explicit form of distribution (16) is now

$$N_{+}(x) = f(x) + c_{+} h(x) + (c_{+}^2 - c_s^2) q(x) \; ,$$

$$N_{\|}(x) = N_0(x) = f(x) - c_s^2 q(x) \; , \qquad (25)$$

$$N_{-}(x) = f(x) - c_{+} h(x) + (c_{+}^2 - c_s^2) q(x) \; . \qquad (26)$$

V. DENSITY PROFILE OBTAINED BY A RECURRENCE METHOD

The evolution equations for velocity states parallel to the interface coupled with the symmetries of the system have been used to determine the form of the density distribution in each site. Now we shall write the evolution of the forward and backward velocity states and obtain the density profile across the interface. It will be compared with simulations in Sec. V D. The existence of local velocities at the interface will be discussed in Sec. V E. Section V F will be devoted to the calculation of pressures and surface tension and their comparison with simulations.

A. Recurrence formulas

In what follows, we will use the notations

$$\kappa(x) = c_{+} h(x) \; , \qquad (27)$$

$$\phi(x) = f(x) + (c_{+}^2 - c_s^2) q(x) \; . \qquad (28)$$

Then

$$N_{+}(x) = \phi + \kappa \; ,$$

$$N_{-}(x) = \phi - \kappa \; . \qquad (29)$$

If we now express the evolution of the forward and backward velocity states [Eq. (6)], stationarity implies that

$$N_{+}(x + c_{+}) = N_{+}''(x) \; , \qquad (30)$$

$$N_{-}(x - c_{+}) = N_{-}''(x) \; . \qquad (31)$$

We note $X = x/c_{+}$ in order to recover a unit space interval. An explicit form of the above equations is

$$\phi(X + 1) + \kappa(X + 1) - \phi(X) - \kappa(X) - \mathcal{G}_{+}(x) = 0 \; , \qquad (32)$$

$$\phi(X - 1) - \kappa(X - 1) - \phi(X) + \kappa(X) + \mathcal{G}_{+}(X) = 0 \; , \qquad (33)$$

where

$$\mathcal{G}_{+}(X) = \Gamma_{+}(X) - \Gamma_{+}(X - r) \qquad (34)$$

and

$$\begin{aligned} \Gamma_{+}(X) &= (N_{-})_X (1 - N_{+})_X (N_{+})_{X+r} (1 - N_{-})_{X+r} \; , \\ &= (\phi - \kappa)_X (1 - \phi - \kappa)_X (\phi + \kappa)_{X+r} \\ &\quad \times (1 - \phi + \kappa)_{X+r} \; . \end{aligned} \qquad (35)$$

The sum of Eqs. (32) and (33) provides a recurrence formula which gives $\kappa(x)$ once the density profile $f(x)$ is known:

$$\kappa(X + 1) = \kappa(X - 1) - \phi(X + 1) + 2\phi(X) - \phi(X - 1) \; . \qquad (36)$$

Notice that away from the interface $\kappa(x)$ tends to zero.

The difference of Eqs. (32) and (33) yields a second equation

$$\phi(X + 1) - \phi(X - 1) + \kappa(X + 1) - 2\kappa(X) + \kappa(X - 1) - 2\mathcal{G}_{+}(X) = 0 \; . \qquad (37)$$

B. Integration of the equations

Equations (36) and (37) form the system that we will solve in order to find the density profile. Before doing so, we shall integrate them and derive two properties of the equilibrium densities, as a test of the validity of our calculations.

Equation (37) writes

$$\mathcal{L}(X) = 0 \; . \qquad (38)$$

We choose two points X_1 and X_2 on each side of the interface, respectively, in the gas and liquid phases. Then

$$\sum_{X=X_1}^{X_2}\mathcal{L}(X)=\phi(X_2+1)+\phi(X_2)+\kappa(X_2+1)$$
$$-\kappa(X_2)-2\left[\sum_{l=0}^{r-1}\Gamma_+(X_2-l)\right]$$
$$-\phi(X_1)-\phi(X_1-1)-\kappa(X_1)$$
$$+\kappa(X_1-1)+2\left[\sum_{l=1}^{r}\Gamma_+(X_1-l)\right].$$

We have $\kappa(X_1)=\kappa(X_2)=0$, $\phi(X_1)=f_1$, and $\phi(X_2)=f_2$. This is also true for the neighboring sites. Thus

$$\sum_{X=X_1}^{X_2}\mathcal{L}(X)=2f_2-2r\Gamma_+(f_2\hat{\mathbf{1}})-2f_1+2r\Gamma_+(f_1\hat{\mathbf{1}})\,. \tag{39}$$

From Eq. (38), this sum must be zero. Then

$$f_2-rf_2^2(1-f_2)^2=f_1-rf_1^2(1-f_1)^2\,. \tag{40}$$

We recognize the pressures of each homogeneous state [20] and find the well known equality

$$p(f_2)=p(f_1)\,. \tag{41}$$

Now we shall do the same with Eq. (36). We have

$$\kappa(X)+\kappa(X+1)=\kappa(X-1)+\kappa(X-2)-\phi(X+2)$$
$$+\phi(X+1)+\phi(X)-\phi(X-1)$$
$$=-\phi(X+2)+\phi(X+1)$$

The second line is obtained by iteration of the recurrence formula up to site X_2. Thus

$$\sum_{X=X_1}^{X_2}[\kappa(X)+\kappa(X+1)]=-\phi(X_2+2)+\phi(X_1+1)\,, \tag{42}$$

which yields

$$2\sum_{X=-\infty}^{+\infty}\kappa(X)=f_1-f_2\,. \tag{43}$$

As a test we will check this property once the density profile will be calculated.

C. Numerical solution

We want to solve numerically the coupled equations (36) and (37). We start from an approached density profile. We have chosen a hyperbolic tangent profile (in fact a double profile in order to have periodic boundary conditions).

The system is solved in two steps.

(i) For a given function κ, Eq. (37) yields a density profile $\phi(X)$. As in [14] we use a spectral scheme

$$\tilde{w}_k^{t+1/2}=(1+\nu k^2)^{-1}[\tilde{w}_k^{t-1/2}-(\widetilde{\mathcal{F}[\phi]})_k^t]\,,$$
$$\tilde{f}_k^{\prime t+1}=\tilde{f}_k^{\prime t}-ik\tilde{w}_k^{t+1/2}\,, \tag{44}$$

where $\mathcal{F}[\phi]$ is the expression which must be made equal to zero [here the left hand side of Eq. (37)]. The notation $\tilde{f}_k$ stands for the Fourier coefficient of $f(x)$. We have chosen this scheme because in our case $\mathcal{F}[\phi]$ is a gradient. Thus classical relaxation schemes do not converge. Using this scheme the density profile will converge from its initial approached value to a new profile until the equation $\mathcal{F}[\phi]=0$ is verified.

(ii) Then a new function κ may be computed from this new density profile using the recurrence formula (36).

The whole process (i) and (ii) is iterated until it converges toward an equilibrium profile. Our convergence criteria is $\|\mathcal{F}[\phi]\|_\infty<10^{-5}$.

This process is unstable toward perturbations of period 2. To avoid the growth of such perturbations, κ is filtered after its calculation:

$$\kappa^f(X)=\tfrac{1}{2}\kappa(X)+\tfrac{1}{4}[\kappa(X+1)+\kappa(X-1)]\,. \tag{45}$$

The filter will introduce perturbations mostly in the regions where the second derivative of κ is the greatest.

This calculation provides the functions $\phi(X)$ and $\kappa(X)$. To compare with numerical measurements on simulations, we need the real density profile $f(X)=\phi(X)-(c_+^2-c_s^2)q(X)$. Indeed q is constrained by the fact that $\hat{\mathbf{N}}$ is a Fermi-Dirac distribution, and can thus be calculated from $\phi(X)$ and $\kappa(X)$.

The detailed calculation of q is given in Appendix C. It may also be found in [21].

D. Results on the density distribution

The theoretical density profile has been calculated for the FCHC liquid-gas model. It has been compared with a measurement on a direct simulation of the liquid-gas model (Fig. 1). The latter was obtained on a $192\times32\times32$ lattice, and averaged over 1000 time steps. The simulation box is very elongated to minimize the fluctuations of the interface. The agreement is much better than the one obtained for the first-order calculation [14].

The forward and backward corrections $\langle N_+-\phi\rangle$ and $\langle N_--\phi\rangle$ have also been measured on the simulation. The

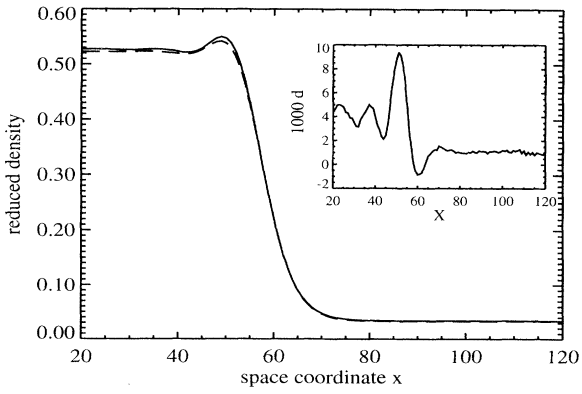

FIG. 1. Comparison between theoretical (dashed line) and numerical (solid line) density profiles. These results have been obtained for the 3D minimal liquid-gas model with an interaction range $r=8$. The inset shows the absolute difference between the profiles.

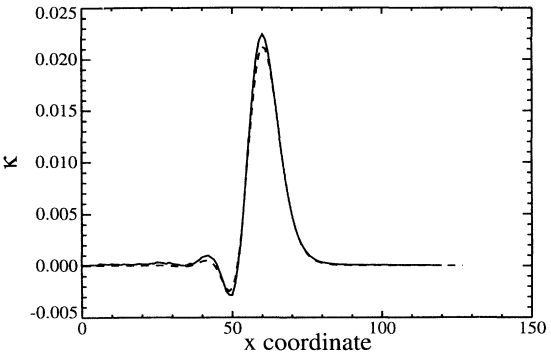

FIG. 2. The norm of the forward and backward corrections in the numerical density distribution (solid lines—both curves are superimposed) compared with the theoretical prediction of κ (dashed line). These results have been obtained for the 3D minimal liquid-gas model with an interaction range $r = 8$.

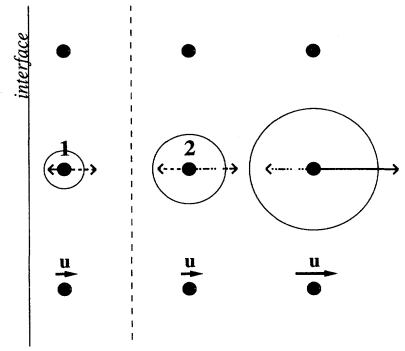

FIG. 3. The departure from an isotropic distribution (circles) is represented for two velocity states orthogonal to the interface, on one line of sites. Velocities with the same modulus are represented with the same type of line (dashed or dashed-dotted). The resulting local velocity is given on the line of sites underneath. Indeed the density distribution is invariant along the direction parallel to the interface. The number of particles propagating from sites 1 to 2 is the same as the number of particles propagating in the opposite direction. The flux across the dashed plane is zero, whereas the local velocity is nonzero in each site.

$\langle\,\rangle$ stands for a spatial and temporal average. We check that these corrections have the same modulus and an opposite sign. They are well fitted by the prediction of κ (Fig. 2), so the distribution form obtained in expression (29) turns out to be correct. As a complementary test we check the relation (43). Indeed we find $2\sum_X \kappa(X) = 0.486$ and $f_{\rm liq} - f_{\rm gas} = 0.490$.

E. Local velocities on the interface

The velocity in a site is defined by

$$\rho u = \sum_i N_i c_{ix} \,. \tag{46}$$

It is directly related to κ by the relation

$$\rho u = \kappa \frac{b c_s^2}{c_+} \,. \tag{47}$$

The reader may be surprised that nonzero local velocities appear at the interface [22,23]. We are indeed looking for a nonpropagating steady density profile. In fact a distinction must be introduced between the local velocity in one site defined by Eq. (46) and the flux of matter across any plane parallel to the interface. A nonzero velocity $\mathbf{u}$ in each site does not prevent the flux from being zero everywhere, as illustrated by Fig. 3. In fact the flux is exactly zero, as Eq. (49) expresses it. To find this equation, notice that from (32) and (33) we have

$$\mathcal{G}_+(X) - \mathcal{G}_+(X+1) = 2\kappa(X+1) - 2\kappa(X) \,. \tag{48}$$

This means that $\mathcal{G}_+(X) + 2\kappa(X)$ is a constant for all values of X, equal to zero from the boundary conditions. We replace $\mathcal{G}_+(X)$ by $-2\kappa(X)$ in Eq. (32) and find

$$\phi(X+1) + \kappa(X+1) = \phi(X) - \kappa(X) \tag{49}$$

which means $N_+(X+1) = N_-(X)$, where N_+ and N_- are the populations at the beginning of the time step; that is, just after propagation. Thus the flux of matter across any plane parallel to the interface is exactly zero.

F. Prediction of surface tension

Once the density distribution is completely known, surface tension may be computed from its mechanical definition [24]

$$\sigma = \int_{-\infty}^{+\infty} [p_n - p_t(x)]dx \,. \tag{50}$$

Due to momentum conservation, p_n does not depend on x. In a previous publication [14], we explained how the normal and tangential pressures p_n and p_t can be derived from the density distribution. Here we have used exactly the same method, except that the density distribution now has the slightly more complicated form of Eqs. (25) and (26). We will only give the results.

The contribution of propagation to the pressure is

$$\begin{aligned} p_n^{\rm GP}(X+\tfrac{1}{2}) &= \sum_{c_{ix}>0} c_{ix}^2 [N_-(X) + N_+(X+1)] \\ &= \frac{b c_s^2}{2} [\phi(X) + \phi(X+1) - \kappa(X) + \kappa(X+1)] \,, \\ p_t^{\rm GP}(X+\tfrac{1}{2}) &= \sum_{\substack{i \\ c_{ix}>0}} c_{iy}^2 [N_-(X) + N_+(X+1)] + \tfrac{1}{2} \sum_{\substack{i \\ c_{ix}=0}} [N_{\|}(X) + N_{\|}(X+1)] \\ &= \frac{b c_s^2}{2} [\phi(X) + \phi(X+1)] - \frac{b c_s^2}{3} c_+^2 [q(X) - q(X+1)] + \frac{b c_s^2}{6} [\kappa(X+1) - \kappa(X)] \,, \end{aligned}$$

and the contribution of interactions is

$$p_n^I(X+\tfrac{1}{2}) = -2\frac{bc_s^2}{2}\sum_{l=0}^{r-1}\Gamma_+(X-l)\,,$$

$$p_t^I(X+\tfrac{1}{2}) = -2\frac{bc_s^2}{6}\sum_{l=0}^{r-1}\Gamma_+(X-l) - r\frac{bc_s^2}{3}[\Gamma_\parallel(X)+\Gamma_\parallel(X+1)]\,.$$

Notice that Eq. (37) is equivalent to

$$p_n(X+\tfrac{1}{2}) - p_n(X-\tfrac{1}{2}) = 0\,, \tag{51}$$

which is a consequence of momentum conservation.

Now surface tension may be calculated as

$$\sigma = \sum_{X=X_1}^{X_2-1}[p_n(X+\tfrac{1}{2}) - p_t(X+\tfrac{1}{2})]\,, \tag{52}$$

where the points X_1 and X_2 are set in homogeneous phases on each side of the interface. Some indications on the calculation are given in Appendix D. We find

$$\sigma = r\frac{bc_s^2}{3}\sum_{X=-\infty}^{+\infty}[2\Gamma_\parallel(X) - \Gamma_+(X) - \Gamma_+(X-r)]\,. \tag{53}$$

In this formula it appears clearly that only the interactions are responsible for the presence of surface tension. The perfect gas contribution is zero.

The origin of surface tension due to interactions can be explained intuitively as follows. In most points on the interface, the interactions in the direction normal to the interface are performed between sites having quite different densities d_1 and d_2, whereas interactions parallel to the interface involve almost identical densities $d \simeq (d_1+d_2)/2$, at least in the center of the interface. As the inequality

$$d_1 d_2 \le \left(\frac{d_1+d_2}{2}\right)^2 \tag{54}$$

holds for any density, the amplitude of the interactions normal to the interface is smaller than the amplitude of interactions parallel to the interface. The contribution of interactions to the pressure appears with a negative sign, and thus the total contribution of p_n^I turns out to be superior to the one of p_t^I.

Figure 4 shows the normal pressure $p_n^{\rm GP} + p_n^I$ and the tangential pressure $p_t^{\rm GP} + p_t^I$ as a function of X. Due to momentum conservation, p_n is exactly constant [Eq. (51)].

Several numerical values of surface tension were obtained from the pressure profiles of Fig. 4 using the rectangle, trapezoidal, and Simpson's integration methods. In all cases we have $\sigma = 1.54$. This result is in agreement with the numerical value $\sigma = 1.4 \pm 0.5$ found from Laplace law on simulations of a cylindrical meniscus [14]. The large error bar is due to the difficulty of measuring precisely the contact angle on the walls.

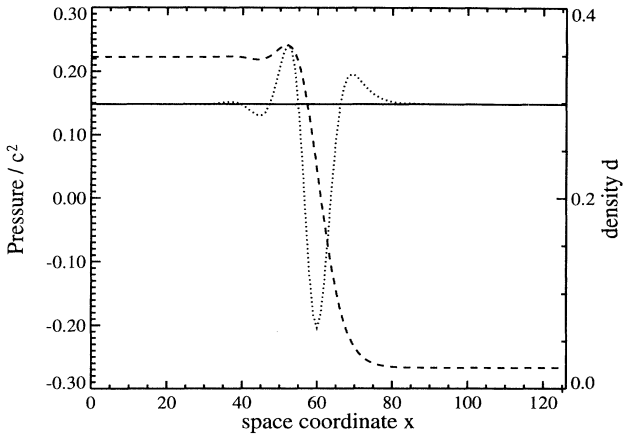

FIG. 4. Normal (solid line) and tangential (dotted line) pressures calculated from the theoretical density distribution, for the 3D minimal liquid-gas model, $r = 8$. The density profile is indicated by a dashed line.

VI. CONCLUSION

We show that even for a model without classical thermodynamics, equilibrium densities can be predicted from purely dynamical arguments.

The method presented here does not assume *a priori* a Fermi-Dirac equilibrium distribution. On the other hand, we assume that the equilibrium distribution exists. All our calculations have been done in the frame of the Boltzmann assumption, i.e., we neglect all the correlations.

We have shown from symmetry arguments that, for the specific orientation of the interface studied here, if the equilbrium distribution exists it is of the form of a Fermi-Dirac one.

From the evolution equations the density profile across the interface has been found. Then a value of surface tension in good agreement with measurements has been predicted. Similar results have been obtained from a third-order asymptotic calculation, which has not been presented here.

Further work should address the case of a curved interface, using an asymptotic calculation. This should allow one to recover Gibbs-Thomson relations, which relate the equilibrium pressures on each side of a curved interface to the radius of curvature and the equilibrium pressure for a flat interface. The usual thermodynamical derivation of these relations [12] is not valid anymore for these lattice-gas models. However, it has been shown numerically that these relations are still verified if a multiplicative coefficient is added into the expression [20].

ACKNOWLEDGMENTS

The authors would like to thank Stéphane Zaleski for his collaboration on this work, and Dan Rothman for stimulating discussions.

TABLE II. Eigenvectors of the linearized collision operator for the FHP model. $\hat{\mathbf{W}}$ is defined only if the number of rest particles $b - b_m$ is nonzero.

Eigenvectors	Eigenvalues
$\hat{\mathbf{1}} = (b - b_m, 1, 1, 1, 1, 1, 1)$	0
$\hat{\mathbf{C}}_x = \{c_{ix}\}_{i=0 \text{ to } 6}$	0
$\hat{\mathbf{C}}_y = \{c_{iy}\}_{i=0 \text{ to } 6}$	0
$\hat{\mathbf{Q}}_{xx} = \{Q_{ixx}\}_{i=0 \text{ to } 6}$ and $\hat{\mathbf{Q}}_{yy} = \{Q_{iyy}\}_{i=0 \text{ to } 6}$	λ
$\hat{\mathbf{V}} = (0, 1, -1, 1, -1, 1, -1)$	ζ
$\hat{\mathbf{W}} = (-b_m/(b - b_m), 1, 1, 1, 1, 1, 1)$	τ

APPENDIX A: RELATIONS ON VELOCITIES FOR THE FHP AND FCHC MODELS

From Eqs. (13) and (11), we have found that

$$\sum_{c_{ix}>0} c_{ix}^2 = \frac{bc_s^2}{2} . \tag{A1}$$

In our calculations we will also need

$$\sum_{\substack{i \\ c_{ix}>0}} c_{iy}^2 = \frac{bc_s^2}{6} ,$$

$$\tfrac{1}{2} \sum_{\substack{i \\ c_{ix}=0}} c_{iy}^2 = \frac{bc_s^2}{3} .$$

These expressions were obtained using

$$\sum_{\substack{i \\ c_{ix}>0}} c_{iy}^2 + \tfrac{1}{2} \sum_{\substack{i \\ c_{ix}=0}} c_{iy}^2 = \tfrac{1}{2} \sum_i c_{iy}^2 = \frac{bc_s^2}{2} \tag{A2}$$

and

$$\sum_{c_{ix}>0} c_{ix}^2 + (D-1) \sum_{\substack{i \\ c_{ix}>0}} c_{iy}^2 = \sum_{c_{ix}>0} \sum_{\beta=1}^{D} c_{i\beta}^2 = b_+ c^2 . \tag{A3}$$

APPENDIX B: GENERAL FORM OF A DISTRIBUTION

A basis of the distribution space may be built using eigenvectors of the linearized collision operator. As there are several way of choosing this basis, in Tables II and III we give the sets of eigenvectors that we used here for the FHP and FCHC models.

Any distribution may be decomposed on this basis. For example, for the FCHC model

$$\hat{\mathbf{N}} = f\hat{\mathbf{1}} + \sum_{\alpha=x}^{t} h_\alpha \hat{\mathbf{C}}_\alpha + \sum_{j=1}^{3} q_j \hat{\mathbf{Q}}_j + \sum_{\substack{\alpha \neq \beta \\ \alpha > \beta}} q'_{\alpha\beta} \hat{\mathbf{Q}}_{i\alpha\beta} + \sum_{j=1}^{10} p_j \hat{\mathbf{V}}_j . \tag{B1}$$

TABLE III. Eigenvectors of the linearized collision operator for the FCHC model.

Eigenvectors	$\hat{\mathbf{1}}$	$\hat{\mathbf{C}}_x$	$\hat{\mathbf{C}}_y$	$\hat{\mathbf{C}}_z$	$\hat{\mathbf{C}}_t$	$\hat{\mathbf{Q}}_1$	$\hat{\mathbf{Q}}_2$	$\hat{\mathbf{Q}}_3$	$\hat{\mathbf{Q}}_{xy}$	$\hat{\mathbf{Q}}_{zt}$	$\hat{\mathbf{Q}}_{xz}$	$\hat{\mathbf{Q}}_{yt}$	$\hat{\mathbf{Q}}_{xt}$	$\hat{\mathbf{Q}}_{yz}$	$\hat{\mathbf{V}}_1$	$\hat{\mathbf{V}}_2$	$\hat{\mathbf{V}}_3$	$\hat{\mathbf{V}}_4$	$\hat{\mathbf{V}}_5$	$\hat{\mathbf{V}}_6$	$\hat{\mathbf{V}}_7$	$\hat{\mathbf{V}}_8$	$\hat{\mathbf{V}}_9$	$\hat{\mathbf{V}}_{10}$
Coordinates	1	1	1	0	0	1	0	0	1	0	0	0	0	0	2	0	2	2	0	0	0	0	0	0
	1	1	−1	0	0	1	0	0	−1	0	0	0	0	0	2	0	2	−2	0	0	0	0	0	0
	1	−1	−1	0	0	1	0	0	1	0	0	0	0	0	2	0	−2	−2	0	0	0	0	0	0
	1	−1	1	0	0	1	0	0	−1	0	0	0	0	0	2	0	−2	2	0	0	0	0	0	0
	1	0	0	1	1	−1	0	0	0	1	0	0	0	0	2	0	0	0	2	2	0	0	0	0
	1	0	0	1	−1	−1	0	0	0	−1	0	0	0	0	2	0	0	0	2	−2	0	0	0	0
	1	0	0	−1	−1	−1	0	0	0	1	0	0	0	0	2	0	0	0	−2	−2	0	0	0	0
	1	0	0	−1	1	−1	0	0	0	−1	0	0	0	0	2	0	0	0	−2	2	0	0	0	0
	1	1	0	1	0	0	1	0	0	0	1	0	0	0	−1	1	−1	0	−1	0	1	0	1	0
	1	1	0	−1	0	0	1	0	0	0	−1	0	0	0	−1	1	−1	0	1	0	1	0	−1	0
	1	−1	0	−1	0	0	1	0	0	0	1	0	0	0	−1	1	1	0	1	0	−1	0	−1	0
	1	−1	0	1	0	0	1	0	0	0	−1	0	0	0	−1	1	1	0	−1	0	−1	0	1	0
	1	0	1	0	1	0	−1	0	0	0	0	1	0	0	−1	1	0	−1	0	−1	0	1	0	1
	1	0	1	0	−1	0	−1	0	0	0	0	−1	0	0	−1	1	0	−1	0	1	0	1	0	−1
	1	0	−1	0	−1	0	−1	0	0	0	0	1	0	0	−1	1	0	1	0	1	0	−1	0	−1
	1	0	−1	0	1	0	−1	0	0	0	0	−1	0	0	−1	1	0	1	0	−1	0	−1	0	1
	1	1	0	0	1	0	0	1	0	0	0	0	1	0	−1	−1	−1	0	0	−1	1	0	0	−1
	1	1	0	0	−1	0	0	1	0	0	0	0	−1	0	−1	−1	−1	0	0	1	−1	0	0	1
	1	−1	0	0	−1	0	0	1	0	0	0	0	1	0	−1	−1	1	0	0	1	1	0	0	1
	1	−1	0	0	1	0	0	1	0	0	0	0	−1	0	−1	−1	1	0	0	−1	1	0	0	−1
	1	0	1	1	0	0	0	−1	0	0	0	0	0	1	−1	−1	0	−1	−1	0	0	−1	−1	0
	1	0	1	−1	0	0	0	−1	0	0	0	0	0	−1	−1	−1	0	−1	1	0	0	−1	1	0
	1	0	−1	−1	0	0	0	−1	0	0	0	0	0	1	−1	−1	0	1	1	0	0	1	1	0
	1	0	−1	1	0	0	0	−1	0	0	0	0	0	−1	−1	−1	0	1	−1	0	0	1	−1	0
eigenvalues	0	0	0	0	0	λ_ν	λ_ν	λ_ν	λ_ν	λ_ν	λ_ν	λ_ν	λ_ν	λ_ν	λ_σ	λ_σ	λ_τ	λ_τ	λ_τ	λ_τ	λ_τ	λ_τ	λ_τ	λ_τ

This general form can be simplified thanks to the system symmetries when a specific problem is studied. For a flat interface, the system is invariant by any reflexion with respect to the x axis, or by any rotation around it. Some particular transformations given in Table IV have been used.

From the resulting relations between the coefficients, we find that the only nonzero coefficients are f, $h_x = h$, and $q_1 = q_2 = q_3 = q$. Noticing that $\hat{\mathbf{Q}}_1+\hat{\mathbf{Q}}_2+\hat{\mathbf{Q}}_3 = \hat{\mathbf{Q}}_{xx}$, with $Q_{i\alpha\beta} = c_{i\alpha}c_{i\beta} - (c^2/D)\delta_{\alpha\beta}$, we obtain the generic form for any distribution having the symmetries of the system

$$\hat{\mathbf{N}} = f\hat{\mathbf{1}} + h\hat{\mathbf{C}}_x + q\hat{\mathbf{Q}}_{xx} + (b - b_m)w\hat{\mathbf{W}} . \tag{B2}$$

APPENDIX C: CALCULATION OF THE SECOND-ORDER CORRECTION

We have seen in Sec. IV C that the collision operator applied to the distribution $\hat{\mathbf{N}}$ is zero, and thus $\hat{\mathbf{N}}$ turns out to be a Fermi-Dirac distribution. This property allows us to express $p = c_+^2 q$ as a function of κ and ϕ. We do not need w, which has been expressed as a function of q by relation (24). We will follow a calculation of Diemer *et al.* and adapt it to our case [21]:

$$N_i = \frac{1}{1 + \exp[\alpha(f,\mathbf{u}) + \beta(f,\mathbf{u})\mathbf{u}\cdot\mathbf{c}_i]} . \tag{C1}$$

We assume there is no more than one zero velocity state. We note $H = \exp[\alpha]$ and $Q = \exp[\beta\mathbf{u}\cdot\mathbf{c}_i]$. Then

$$N_+ = \frac{1}{1+HQ}, \quad N_{\|} = N_0 = \frac{1}{1+H}, \quad N_- = \frac{1}{1+H/Q} . \tag{C2}$$

On the other hand [Eq. (25)], the density distribution was found equal to

$$\begin{aligned} N_+(x) &= f(x) + c_+h(x) + (c_+^2 - c_s^2)q(x) = \phi + \kappa , \\ N_{\|}(x) = N_0 &= f(x) - c_s^2 q(x) = \phi - c_+^2 q , \\ N_-(x) &= f(x) - c_+h(x) + (c_+^2 - c_s^2)q(x) = \phi - \kappa . \end{aligned} \tag{C3}$$

The elimination of H and Q will provide $p = c_+^2 q$ as a function of κ and ϕ.

The number of forward velocities ($c_{ix} > 0$) is $b_+ = (b_m c^2/2Dc_+^2)$. Then ϕ may be expressed as

$$2\phi = \frac{1}{1+HQ} + \frac{1}{1+H/Q} . \tag{C4}$$

This expression may be seen as a linear equation for the variable $Q + 1/Q$. The solution is

$$Q + \frac{1}{Q} = \frac{2[\phi(1+H^2) - 1]}{H(1-2\phi)} . \tag{C5}$$

A second equation is given by

$$2\kappa = \frac{1}{1+HQ} - \frac{1}{1+H/Q} . \tag{C6}$$

If we take the square of this equation, and use the relation

$$(Q - 1/Q)^2 = (Q + 1/Q)^2 - 4 , \tag{C7}$$

TABLE IV. Transformations used to find the general form of any distribution having the symmetries of the system, in three dimensions for the FCHC model. The invariance by a transformation of the second column implies some relations between the coefficients of $\hat{\mathbf{N}}$ given in the last column.

Transformation type	Transformation definition in 4D	Conclusion
reflection	$S_1 = \begin{pmatrix} 1 & 0 & 0 & 0 \\ 0 & -1 & 0 & 0 \\ 0 & 0 & 1 & 0 \\ 0 & 0 & 0 & 1 \end{pmatrix}$	$q'_{xy} = q'_{yz} = q'_{yt} = h_y = p_4 = p_8 = 0$
reflection	$S_2 = \begin{pmatrix} 1 & 0 & 0 & 0 \\ 0 & -1 & 0 & 0 \\ 0 & 0 & -1 & 0 \\ 0 & 0 & 0 & -1 \end{pmatrix}$	$q'_{xz} = q'_{yz} = q'_{zt} = h_z = p_5 = p_9 = 0$
reflection	$S_3 = \begin{pmatrix} 1 & 0 & 0 & 0 \\ 0 & 1 & 0 & 0 \\ 0 & 0 & 1 & 0 \\ 0 & 0 & 0 & -1 \end{pmatrix}$	$q'_{zt} = q'_{yt} = q'_{xt} = h_t = p_6 = p_{10} = 0$
rotation	$R_1 = \begin{pmatrix} 1 & 0 & 0 & 0 \\ 0 & 0 & 1 & 0 \\ 0 & -1 & 0 & 0 \\ 0 & 0 & 0 & 1 \end{pmatrix}$	$q_1 = q_2$ $3p_1 = p_2$
rotation	$R_2 = \begin{pmatrix} 1 & 0 & 0 & 0 \\ 0 & 0 & 0 & 1 \\ 0 & 0 & 1 & 0 \\ 0 & -1 & 0 & 0 \end{pmatrix}$	$q_1 = q_3$ $3p_1 = -p_2$

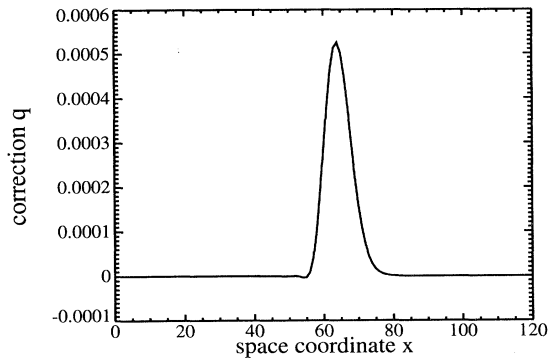

FIG. 5. Second-order correction q to the occupation distribution, obtained for the 3D minimal liquid-gas model, with $r = 8$.

Q appears again only by the term $Q + 1/Q$. We report the value of Q given by Eq. (C5) into Eq. (C6). We find

$$\kappa^2(1 - H^2) = [\phi(1 + H) - 1][\phi(1 - H) - 1] . \quad \text{(C8)}$$

It is convenient to note

$$p \equiv c_+^2 q = \phi - \frac{1}{1 + H} . \quad \text{(C9)}$$

The elimination of H between expressions (C9) and (C8) leads to a polynomial expression of p:

$$\mathcal{P}[p] = a_0 + a_1 p + a_2 p^2 = 0 , \quad \text{(C10)}$$

with

$$\begin{aligned} a_0 &= \kappa^2(1 - 2\phi) , \\ a_1 &= -2[\phi(1 - \phi) - \kappa^2] , \\ a_2 &= 1 - 2\phi . \end{aligned} \quad \text{(C11)}$$

Note that in the general case we should have found a cubic equation. Here by chance it turns out to be only quadratic. The interesting root is

$$p = \frac{\kappa^2(1 - 2\phi)}{\phi(1 - \phi) - \kappa^2 + \sqrt{[\phi^2 - \kappa^2][(1 - \phi)^2 - \kappa^2]}} . \quad \text{(C12)}$$

We give the solution in this form in order to avoid the denominator becoming zero at $\phi = \frac{1}{2}$

Figure 5 shows the resulting correction $q(X) = p(X)/c_+^2$.

Once the correction $q(X)$ is known, the exact density profile

$$f(X) = \phi(X) - (c_+^2 - c_s^2) q(X) \quad \text{(C13)}$$

may be compared with measurements on direct simulations of the liquid-gas model.

APPENDIX D: SURFACE TENSION EXPRESSION

We take two points with $X = X_1$ and $X = X_2$, respectively, in the gas and liquid phases. The surface tension is defined by

$$\sigma = \sum_{X=X_1}^{X_2-1} [p_n(X + \tfrac{1}{2}) - p_t(X + \tfrac{1}{2})] . \quad \text{(D1)}$$

The contribution of perfect gas pressures is

$$p_n^{\mathrm{GP}}(X + \tfrac{1}{2}) - p_t^{\mathrm{GP}}(X + \tfrac{1}{2}) = \frac{bc_s^2}{3}[\kappa(X + 1) - p'(X + 1) - \kappa(X) + p'(X)] . \quad \text{(D2)}$$

Then

$$\sum_{X=X_1}^{X_2-1} [p_n^{\mathrm{GP}}(X + \tfrac{1}{2}) - p_t^{\mathrm{GP}}(X + \tfrac{1}{2})] = \frac{bc_s^2}{3}[\kappa(X_2) - p'(X_2) - \kappa(X_1) + p'(X_1)] = 0 . \quad \text{(D3)}$$

The contribution of interactions is

$$p_n^I(X + \tfrac{1}{2}) - p_t^I(X + \tfrac{1}{2}) = -2\frac{bc_s^2}{3}\sum_{l=0}^{r-1}\Gamma_+(X - l) + r\frac{bc_s^2}{3}[\Gamma_\parallel(X) + \Gamma_\parallel(X + 1)] . \quad \text{(D4)}$$

We will sum separately the two terms. We call Γ_+^{gas} and Γ_+^{liq} the values of $\Gamma_+(X) = \Gamma_\parallel(X) = \Gamma_-(X)$ in the gas and liquid phases. Thus

$$\begin{aligned} \sum_{X=X_1}^{X_2-1}\sum_{l=0}^{r-1}\Gamma_+(X - l) &= \sum_{X=X_1}^{X_2-r} r\Gamma_+(X) + \sum_{n=1}^{r-1}(\Gamma_+^{\mathrm{liq}} + \Gamma_+^{\mathrm{gas}}) \\ &= \frac{r}{2}\sum_{X=X_1}^{X_2-r}\Gamma_+(X) + \frac{r}{2}\sum_{X=X_1+r}^{X_2}\Gamma_+(X + 1) + \frac{r(r-1)}{2}(\Gamma_+^{\mathrm{liq}} + \Gamma_+^{\mathrm{gas}}) \\ &= \frac{r}{2}\sum_{X=X_1+r}^{X_2-r}[\Gamma_+(X) + \Gamma_+(X + 1)] + \frac{r^2}{2}(\Gamma_+^{\mathrm{liq}} + \Gamma_+^{\mathrm{gas}}) + \frac{r(r-1)}{2}(\Gamma_+^{\mathrm{liq}} + \Gamma_+^{\mathrm{gas}}) \end{aligned}$$

and

$$\sum_{X=X_1}^{X_2-1} [\Gamma_\parallel(X) + \Gamma_\parallel(X+1)] = \sum_{X=X_1+r}^{X_2-r} 2\Gamma_\parallel(X) + (2r-1)(\Gamma_+^{\rm liq} + \Gamma_+^{\rm gas}). \tag{D5}$$

Then we find

$$\sigma = r\frac{bc_s^2}{3} \sum_{X=X_1+r}^{X_2-r} [2\Gamma_\parallel(X) - \Gamma_+(X) - \Gamma_+(X-r)] \,. \tag{D6}$$

The limits of the sum can be sent respectively to $-\infty$ and $+\infty$ without changing the result.

[1] Uriel Frisch, B. Hasslacher, and Yves Pomeau, Phys. Rev. Lett. **56**, 1505 (1986).

[2] U. Frisch, D. d'Humières, B. Hasslacher, P. Lallemand, Y. Pomeau, and J. P. Rivet, Comp. Syst. **1**, 649 (1987).

[3] Bracy H. Elton, C. David Levermore, and Garry H. Rodrigue, SIAM J. Numer. Anal. (to be published).

[4] C. Appert and S. Zaleski, Phys. Rev. Lett. **64**, 1 (1990).

[5] Patrick Grosfils, Jean-Pierre Boon, and Pierre Lallemand, Phys. Rev. Lett. **68**, 1077 (1992).

[6] D. H. Rothman and J. M. Keller, J. Stat. Phys. **52**, 1119 (1988).

[7] Pascal Bellon, Phys. Rev. B **45**, 7517 (1992).

[8] E. Salomon, P. Bellon, F. Soisson, and G. Martin, Phys. Rev. B **45**, 4582 (1992).

[9] F. Soisson, P. Bellon, and G. Martin, Phys. Rev. B **46**, 11 332 (1992).

[10] C. Appert, D. d'Humières, and S. Zaleski, C. R. Acad. Sci. Paris. II **316**, 569 (1993).

[11] Xiaowen Shan and Hudong Chen, Phys. Rev. E **49**, 2941 (1994).

[12] Y. Rocard, *Thermodynamique* (Masson, Paris, 1952).

[13] C. Adler, D. d'Humières, and D. H. Rothman, J. Phys. I France **4**, 29 (1994).

[14] C. Appert, V. Pot, and S. Zaleski, in *Pattern Formation and Lattice-Gas Automata*, edited by A. Lawniczak and R. Kapral, Fields Institute Communications (American Mathematical Society, Providence, RI, in press).

[15] H. J. Bussemaker and M. H. Ernst, J. Stat. Phys. **68**, 431 (1992).

[16] M. Gerits, M. H. Ernst, and D. Frenkel, Phys. Rev. E **48**, 988 (1993).

[17] C. Appert, D. Rothman, and S. Zaleski, Physica D **47**, 85 (1991).

[18] D. d'Humières, P. Lallemand, and U. Frisch, Europhys. Lett. **2** 291 (1986).

[19] J. A. Somers and P. C. Rem, Lecture Notes Phys. **398**, 59 (1992).

[20] C. Appert and S. Zaleski, J. Phys. France II **3**, 309 (1993).

[21] K. Diemer, K. Hunt, S. Chen, T. Shimomura, and G. Doolen, in *Lattice Gas Methods for Partial Differential Equations*, edited by G. Doolen *et al.* (Addison-Wesley Publishing Co., 1989), pp. 137–177.

[22] Rémi Cornubert, Dominique d'Humières, and David Levermore, Physica D **47**, 241 (1991).

[23] Andrew K. Gunstensen, Ph.D. thesis, Massachusetts Institute of Technology, 1992.

[24] Rowlinson and Widom, *Molecular Theory of Capillarity* (Clarendon, Oxford, 1982).